

ORIGINAL RESEARCH

High-Resolution Transthoracic Echocardiography Accurately Detects Pulmonary Arterial Pressure and Decreased Right Ventricular Contractility in a Mouse Model of Pulmonary Fibrosis and Secondary Pulmonary Hypertension

Thomas S. Hansen, MBBS, PhD; Kristen J. Bubb , PhD; Gabriele G. Schiattarella , MD, PhD; Martin Ugander , MD, PhD; Timothy C. Tan , MBBS, PhD; Gemma A. Figtree , MBBS, PhD

BACKGROUND: To date, assessment of right ventricular (RV) function in mice has relied extensively on invasive measurements. Echocardiographic advances have allowed adaptation of measures used in humans for serial, noninvasive RV functional assessment in mice. We evaluated the diagnostic performance of tricuspid annular plane systolic excursion (TAPSE), RV peak systolic myocardial velocity (s'), RV myocardial performance index (MPI), and RV fractional area change (FAC) in a mouse model of pulmonary hypertension.

METHODS AND RESULTS: Echocardiography was performed on mice at baseline and 3 weeks after induction of pulmonary hypertension using inhaled bleomycin or saline, including adapted measures of TAPSE, s' , MPI, and FAC. RV systolic pressure was measured by invasive catheterization, and RV contractility was measured as the peak slope of the RV systolic pressure recording (maximum change pressure/change time). Postmortem morphological assessment of RV hypertrophy was performed. RV systolic pressure was elevated and maximum change pressure/change time was reduced in bleomycin versus control ($n=8$; $P=0.002$). Compared with controls, bleomycin mice had reduced TAPSE (0.79 ± 0.05 versus 1.06 ± 0.04 mm; $P=0.003$), s' (21.3 ± 1.2 versus 29.2 ± 1.3 mm/s; $P<0.001$), and FAC ($20.3\pm 0.7\%$ versus $31.0\pm 1.3\%$; $P<0.001$), whereas MPI was increased (0.51 ± 0.03 versus 0.37 ± 0.01 ; $P=0.006$). All measures correlated with RV systolic pressure and maximum change pressure/change time. Intraobserver and interobserver variability were minimal. Receiver operating characteristic curves demonstrated that TAPSE (<0.84 mm), s' (<23.3 mm/s), MPI (0.42), and FAC ($<23.3\%$) identified maximum change pressure/change time ≤ 2100 mmHg/s with high accuracy.

CONCLUSIONS: TAPSE, s' , MPI, and FAC are measurable consistently using high-resolution echocardiography in mice, and are sensitive and specific measures of pulmonary pressure and RV function. This validation opens the opportunity for serial noninvasive measures in mouse models of pulmonary hypertension, enhancing the statistical power of preclinical studies of novel therapeutics.

Key Words: bleomycin ■ echocardiography ■ mouse model ■ pulmonary hypertension ■ right ventricle

Correspondence to: Gemma A. Figtree, MBBS, PhD, Kolling Institute, University of Sydney and Royal North Shore Hospital St Leonards, New South Wales 2065, Australia. Email: gemma.figtree@sydney.edu.au

For Sources of Funding and Disclosures, see page 11.

© 2022 The Authors. Published on behalf of the American Heart Association, Inc., by Wiley. This is an open access article under the terms of the [Creative Commons Attribution-NonCommercial-NoDerivs](https://creativecommons.org/licenses/by-nc-nd/4.0/) License, which permits use and distribution in any medium, provided the original work is properly cited, the use is non-commercial and no modifications or adaptations are made.

JAHA is available at: www.ahajournals.org/journal/jaha

CLINICAL PERSPECTIVE

What Is New?

- Herein, measures of tricuspid annular plane systolic excursion, right ventricular myocardial performance index, and right ventricular fractional area change are measurable consistently using high-resolution echocardiography in mice and are sensitive and specific measures of pulmonary pressure and right ventricular function.

What Are the Clinical Implications?

- This validation opens the opportunity for serial noninvasive measures in mouse models of pulmonary hypertension, accelerating the translation of novel therapeutics targeting right ventricular function and remodeling, key to prognosis in humans.

Nonstandard Abbreviations and Acronyms

dP/dt max	maximum change pressure/change time
ET	ejection time
FAC	fractional area change
MPI	myocardial performance index
PAT	pulmonary acceleration time
PH	pulmonary hypertension
RVSP	right ventricular systolic pressure
s'	right ventricular peak systolic myocardial velocity
TAPSE	tricuspid annular plane systolic excursion

Pulmonary hypertension (PH) is a heterogeneous disease defined clinically by a mean pulmonary artery pressure ≥ 25 mmHg, demonstrated by right-sided heart catheterization at rest.¹ The World Health Organization classification of PH categorizes PH into 5 groups, according to underlying pathophysiology, that extends from primary pulmonary arterial hypertension, to those secondary to a range of pulmonary and left-sided heart abnormalities. Common to all of these subtypes of PH is chronic pressure overload driving right ventricular (RV) hypertrophy and ultimately RV failure.² It has been shown that it is the resilience or failure of the RV that most closely associates with clinical outcome.³

Given the importance of RV function in determining outcomes in patients with all forms of PH, improved techniques for serial measures of RV hemodynamics in preclinical models are critical. However, until now,

assessment of PH and RV function has relied predominantly on invasive right-sided heart catheterization. This can typically only be performed as a terminal procedure. As a result, longitudinal data to monitor disease progression are missed or require separate groups of mice for evaluation at each longitudinal time point. Echocardiographic assessment of the RV in humans with PH has multiple well-defined surrogate measures that reflect the severity of RV dysfunction, including tricuspid annular plane systolic excursion (TAPSE), RV peak systolic myocardial velocity (s'), RV myocardial performance index (MPI), and RV fractional area change (FAC). In mouse models, the ability to reliably detect RV dysfunction by echocardiography has been limited in the past by image quality. With advances in the temporal and spatial resolution of state-of-the-art preclinical imaging, it is now feasible to obtain high-quality images of RV function in mice. However, comprehensive application of these noninvasive measures in murine models of PH with invasive correlates of pressure and contractile function have yet to be performed. In the present study, we apply advanced, high-resolution echocardiographic measures of RV function in mice, and for the first time, correlate these with invasive measures of pulmonary arterial pressure and RV contractile function in a model of group III PH.

METHODS

The data that support the findings of this study are available from the corresponding author on reasonable request.

The study was approved by the Northern Sydney Local Health District Animal Ethics Committee (approval numbers RESP/17/229 and RESP/18/101) and conforms to the National Health and Medical Research Council of Australia's *Code of Practice for the Care and Use of Animals for Scientific Purposes*. Experiments were performed in male C57BL6/J mice, aged 8 to 16 weeks.

Bleomycin Model

Bleomycin sulphate (Sigma-Aldrich) was dissolved in sterile 0.9% NaCl. Under light anesthesia, C57BL6 mice were administered a single oropharyngeal aspiration of bleomycin (2 mg/kg body weight) or saline control in a randomized manner.⁴

Echocardiography

Transthoracic echocardiography was performed at 3 weeks, immediately before euthanasia. In a subset of mice, baseline echocardiography was also performed to allow for longitudinal evaluation. Echocardiography was performed in a blinded manner with the Vevo3100

imaging system (VisualSonics Inc, Toronto, Ontario, Canada) equipped with a 40-MHz probe (MS400) on lightly anesthetized mice using 1.5% isoflurane. Heart rates were maintained above 400 beats per minute. The heart was imaged in the parasternal short axis with pulse-wave Doppler at the basal level of the short axis, to measure pulmonary acceleration time (PAT) and pulmonary ejection time (ET), surrogate measures of pulmonary artery pressure. The diameter of the RV anterior wall (RV area wall diastole) was measured by M-mode in the parasternal long axis. *4-Chamber*: Our 4-chamber echocardiography protocol for assessment of the right ventricle was established to emulate clinical

imaging guidelines for humans written by the American Society of Echocardiography.⁵ An apical 4-chamber view was acquired to assess TAPSE, s' , MPI, and FAC. Briefly, a focused right-sided heart 4-chamber view was obtained by placing the transducer midway between a traditional apical 4-chamber and subcostal view. TAPSE, s' , and MPI were obtained by using M-mode and tissue Doppler, at the tricuspid annulus of the RV free wall. TAPSE (M-mode) measured the total displacement of the tricuspid annulus from end systole to end diastole (Figure 1). S' (tissue Doppler) was measured as the peak systolic velocity. MPI (tissue Doppler) was calculated by measuring the tricuspid

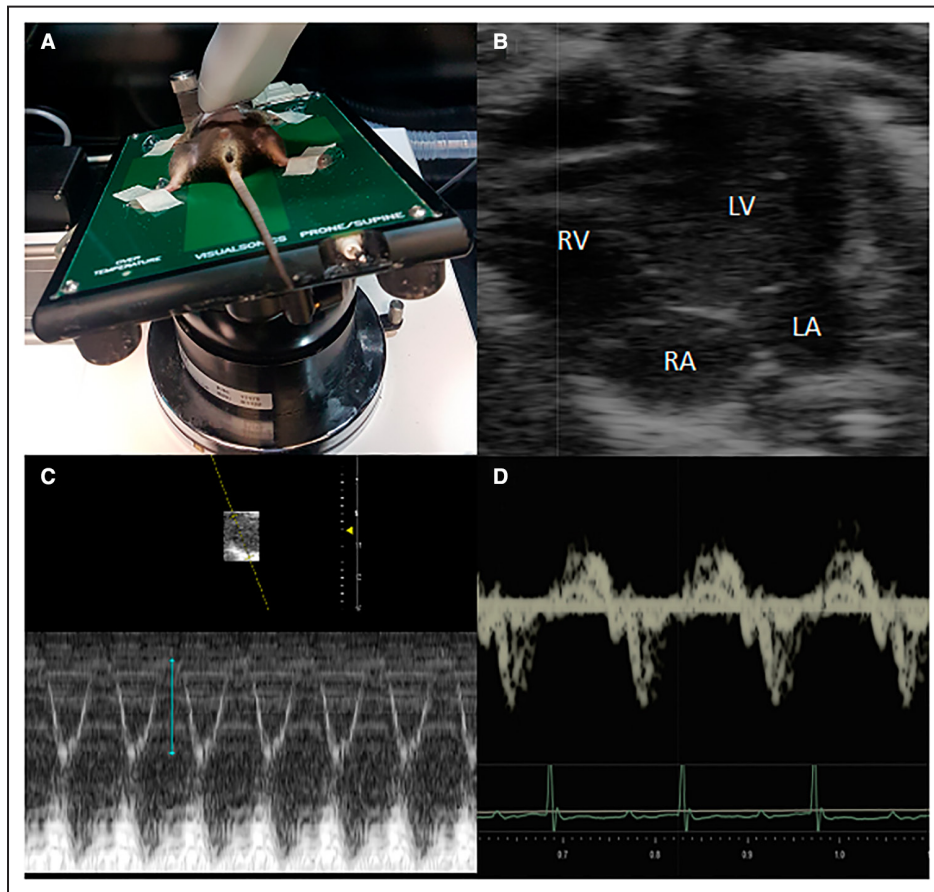


Figure 1. Measurement of TAPSE, RV peak systolic myocardial velocity (s'), MPI, and FAC.

A, MX400 transducer probe was placed midway between a traditional apical 4-chamber and subcostal view to obtain an RV-focused view. **B**, End-diastole and end-systole B-mode images were obtained, allowing calculation of RV FAC= $(RV\ end\ diastolic\ area\ [RVEDA]-RV\ end\ systolic\ area)/RVEDA$. **C**, TAPSE: In the 4-chamber view using M-mode, the gate is placed over the lateral tricuspid valve or tricuspid annular plane. An image is acquired, demonstrating the excursion of the tricuspid valve from diastole to systole. Three measurements in consecutive cardiac cycles are taken of this excursion (peak to trough) and averaged. Measurements were analyzed using Vevo3100 echocardiographic postprocessing software. **D**, S' and MPI: Pulsed-wave tissue Doppler placed in the lateral tricuspid annulus allowed measurement of s' , ET (from end of IVCT to beginning of IVRT), and TCO, defined as ET+IVCT+IVRT. From this, MPI was calculated using the equation $MPI=(TCO-ET)/ET$. ET indicates ejection time; FAC, fractional area change; IVCT, isovolumic contraction time; IVRT, isovolumic relaxation time; LA, left atrial; LV, left ventricular; MPI, myocardial performance index; RA, right atrial; RV, right ventricular; TAPSE, tricuspid annular plane systolic excursion; and TCO, tricuspid closure-opening time.

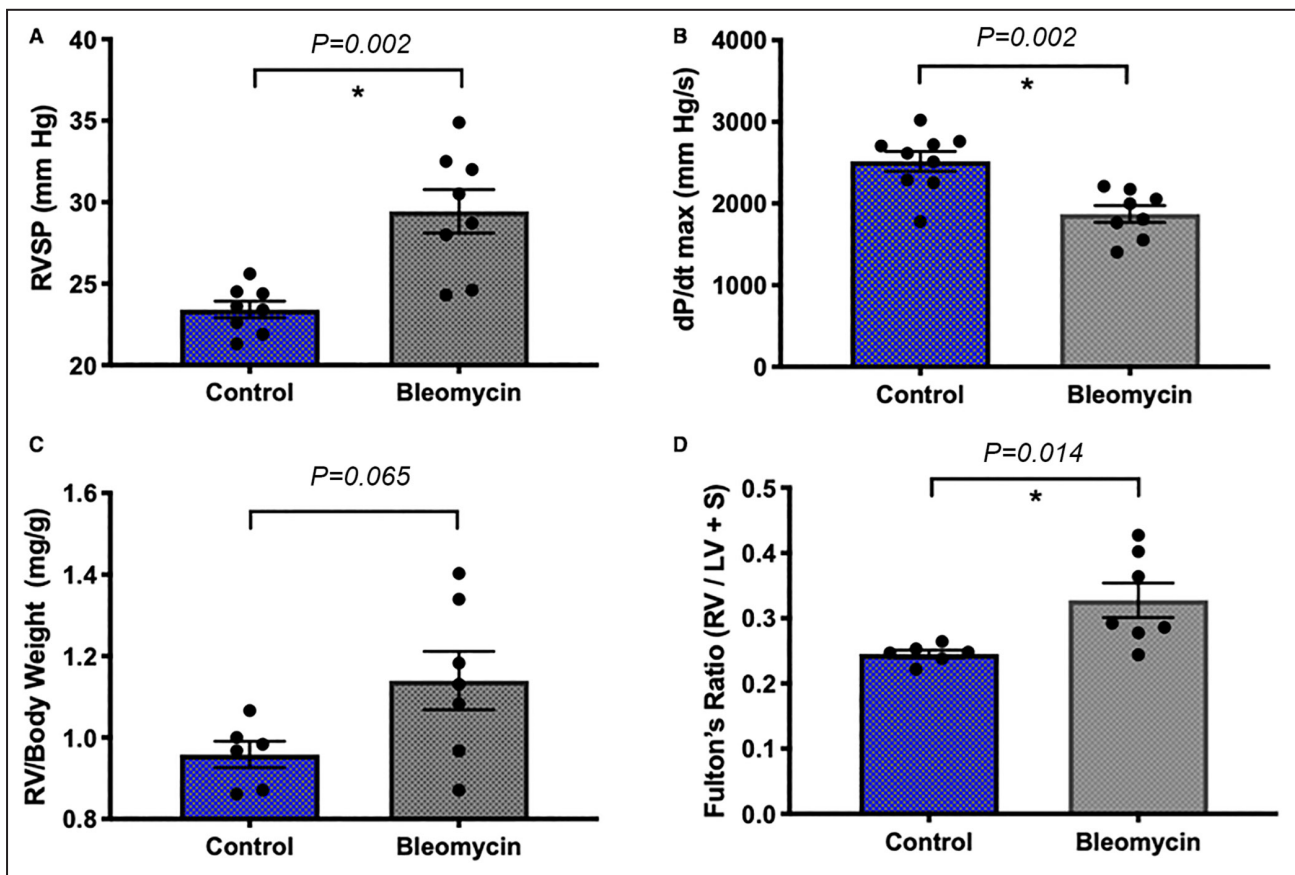


Figure 2. Hemodynamic and RV morphometric measures in control and bleomycin mice.

Bleomycin induced a significant increase in RVSP (A) and decrease in maximum change pressure/change time (dP/dt max) (B) compared with saline control, as measured by invasive hemodynamics (control, n=8; BLEO, n=8). C, RV/body weight ratio (control, n=6; BLEO, n=7). D, Fulton ratio (control, n=6; BLEO, n=7). Data are presented as mean±SEM. Statistical analysis was performed using nonparametric Mann-Whitney tests. BLEO indicates bleomycin; LV+S, left ventricle plus septum; RV, right ventricular; and RVSP, RV systolic pressure.

closure-opening time and ET, and then using the equation: $MPI = (\text{tricuspid closure-opening time} - ET) / ET$ (Figure 1). The RV endocardial border of the 4-chamber view was traced in end systole and end diastole, to give the RV end-systolic area and RV end-diastolic area. FAC was calculated as $FAC = (\text{RV end-diastolic area} - \text{RV end-systolic area}) / \text{RV end-diastolic area}$. A total of 2 of 18 mice (11%) were excluded from analysis because of poor image quality. All measurements were performed offline using the VevoLab Analysis Software (FUJIFILM VisualSonics Inc, Toronto, Ontario, Canada).

Invasive Hemodynamics

Mice were anesthetized with isoflurane (1%–1.5% in O_2 ; 0.8L/min). Body temperature was maintained at 36.5 to 37 °C, and respiration rate was maintained between 80 and 100 breaths/min. The right jugular vein was ligated and a 1.4F pressure catheter (SPR-671; Millar) was advanced via an incision into the RV to measure RV systolic pressure (RVSP). RVSP and heart rate were recorded using a Power-Lab data

acquisition system (Version 7; AD Instruments, Bella Vista, Australia). Maximum change pressure/change time (dP/dt max) was measured from the average maximal height of the first derivative of the pressure waveforms. In a second cohort of mice, a 1F pressure-volume catheter (PVR 1045; Millar) was placed in the RV using an identical closed-chest procedure. This was connected to a Millar Mikro-tip Pressure Volume System (AD Instruments) and recorded using Labchart software. The pressure signal was manually calibrated using an external sphygmomanometer, and volume was calibrated by placing mouse blood (extracted at conclusion of recording) into known volume channels of a mouse calibration cuvette (AD Instruments).

Postmortem Tissue Collection

The mouse was euthanized, and heart and lungs were removed. The RV free wall was separated from the left ventricle and septum, and each weighed, allowing calculation of the Fulton ratio (RV/left ventricle and septum).

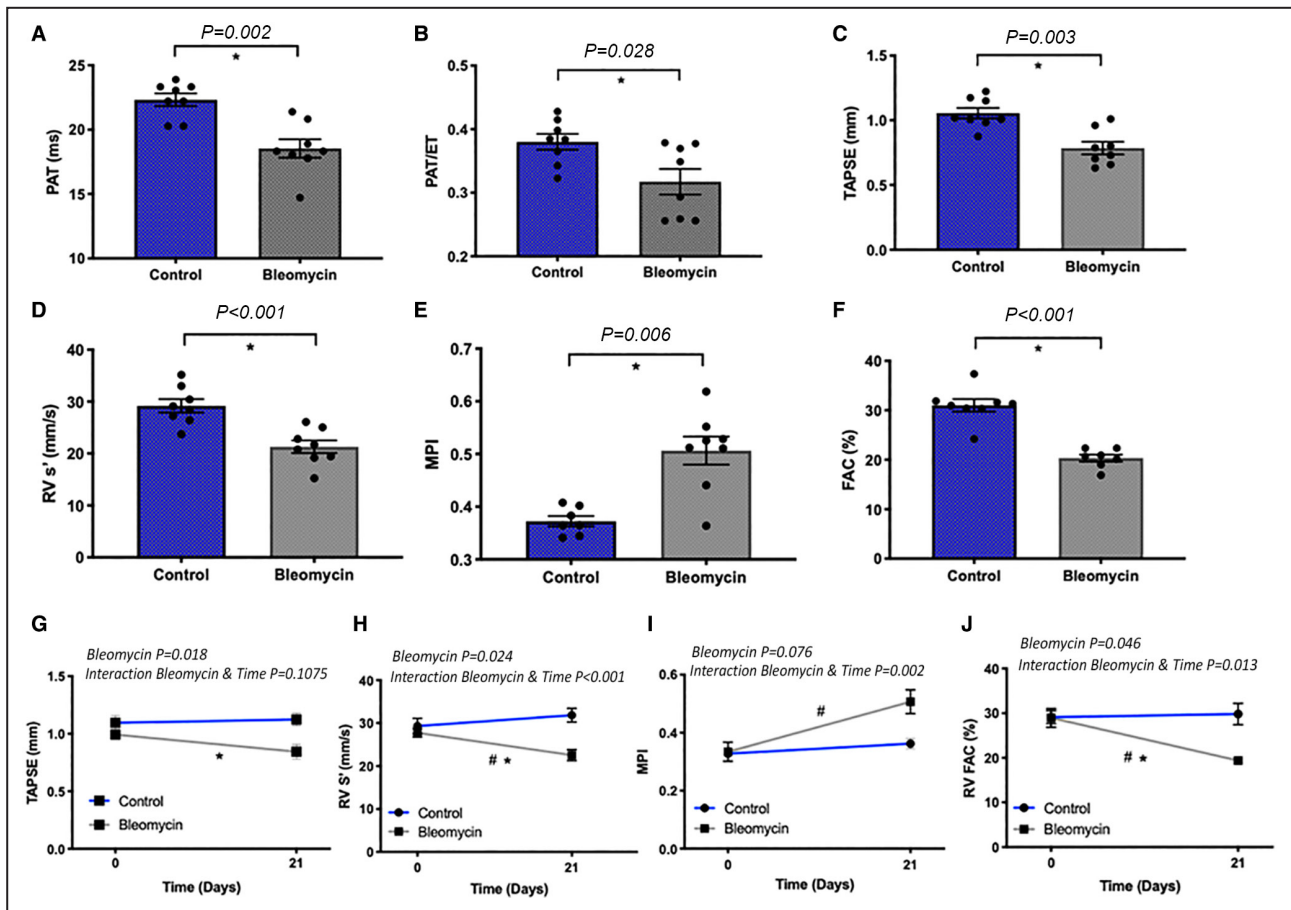


Figure 3. Application of murine echocardiographic measures of pulmonary pressure and novel echocardiographic measures of RV function in BLEO model of pulmonary hypertension.

A, PAT (control, n=8; BLEO, n=8). **B,** PAT/ET was nonsignificantly different between control and BLEO mice (control, n=8; BLEO, n=8). **C,** TAPSE in control and BLEO-treated mice (control, n=8; BLEO, n=8). **D,** RV peak systolic myocardial velocity (s') in control and BLEO-treated mice (control, n=8; BLEO, n=8). **E,** MPI in control and BLEO-treated mice (control, n=7; BLEO, n=8). **F,** FAC in control and BLEO-treated mice (control, n=8; BLEO, n=7). Longitudinal assessment of TAPSE (**G**), s' (**H**), MPI (**I**), and FAC (**J**) in control and BLEO mice. Data are presented as mean±SEM. Statistical analysis was performed using nonparametric Mann-Whitney tests for **A** through **F** and by 2-way repeated-measures ANOVA for **G** through **J**. * $P<0.05$, statistically significant BLEO vs control; # $P<0.05$, statistical interaction for treatment and time. BLEO indicates bleomycin; ET, ejection time; FAC, fractional area change; MPI, myocardial performance index; PAT, pulmonary acceleration; RV, right ventricular; and TAPSE, tricuspid annular plane systolic excursion.

Statistical Analysis

Statistical analysis was performed using GraphPad Prism 7 software. Experimental groups were analyzed by the nonparametric Mann-Whitney test. Values are presented as mean±SEM. The Pearson correlation coefficient was used to evaluate linear correlations, and expressed as its square (R^2). Interobserver and intraobserver variability were measured by 2 independent observers (T.S.H, K.J.B) on 2 separate occasions. Intraobserver and interobserver results were analyzed using the Student paired t test and the intraclass correlation coefficient. Bland-Altman plots were used to plot the differences of TAPSE, s', MPI, and FAC measured by the 2 observers (T.S.H, K.J.B) against their average. Receiver operating characteristic analysis was performed, with optimal cutoff values identified using the Youden index.

RESULTS

Invasive Hemodynamics and RV Morphometry in a Bleomycin Model of Group III PH

Bleomycin-induced pulmonary fibrosis and secondary pulmonary hypertension were characterized by increased pulmonary artery and RV systolic pressures, which led to a pressure afterload-induced RV hypertrophy, and consequently an increase in the measured ratio of RV to left ventricle and septal weight (Fulton ratio). RVSP measured by invasive right-sided heart catheterization was increased in bleomycin mice (29.44 ± 1.3 mmHg; n=8) compared with saline controls (23.41 ± 0.5 mmHg; n=8; $P<0.002$) (Figure 2A). dP/dt max was decreased in bleomycin mice (1872 ± 102 mmHg/s

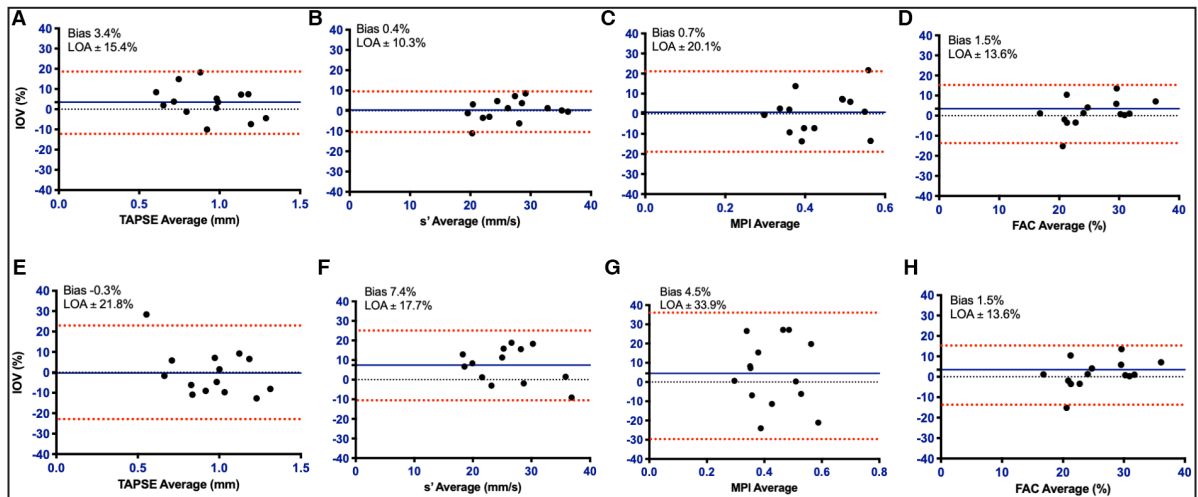


Figure 4. Interobserver and intraobserver variability in novel murine measurements of RV function.

Bland-Altman analysis demonstrating the intraobserver variability in echocardiographic measures of TAPSE (A), RV peak systolic myocardial velocity (s') (B), MPI (C), and FAC (D), and interobserver variability in echocardiographic measures of TAPSE (E), s' (F), MPI (G), and FAC (H) ($n=14$ for all). The analysis was performed on images acquired at 3 weeks in a blinded manner by 2 individuals (T.S.H, K.J.B.) experienced in echocardiographic analysis. To assess intraobserver variability, a period of 4 weeks between serial analysis was observed. LOA is shown with a dotted red line. Bias is demonstrated with a solid blue line. Bland-Altman plots demonstrate the intraobserver/interobserver differences against their average. FAC indicates fractional area change; LOA, limits of agreement; MPI, myocardial performance index; RV, right ventricular; and TAPSE tricuspid annular plane systolic excursion.

[$n=8$] versus 2518 ± 121 mmHg/s [$n=9$]; $P < 0.002$) (Figure 2B). RV/body weight ratio trended toward being increased in bleomycin mice (1.14 ± 0.1 [$n=7$] versus 0.96 ± 0.1 [$n=6$]; $P=0.06$) (Figure 2C), reflecting bleomycin-induced RV hypertrophy, which translated to an increase in the Fulton ratio (0.33 ± 0.03 [$n=7$] versus 0.25 ± 0.01 [$n=6$]; $P < 0.02$) (Figure 2D).

Echocardiographic Parameters of Pulmonary Pressure and RV Function

Given the normal absence of tricuspid regurgitant jets in mice, alternative noninvasive measures of pulmonary pressures have been used. PH is known to result in premature pulmonary valve closure, and more rapid increase to peak velocity across the pulmonary valve, resulting in a shorter PAT and ET.⁶ PAT and ET have been shown to closely correlate with RVSP in a murine model of group III PH.⁷ Similarly to these prior studies, we found that PAT was reduced in bleomycin mice (18.5 ± 0.8 ms; $n=8$) compared with control (22.3 ± 0.5 ms; $n=8$; $P < 0.002$) (Figure 3A). PAT/ET was also reduced in bleomycin mice (0.26 ± 0.02 [$n=8$] versus 0.32 ± 0.01 [$n=8$]; $P=0.028$) (Figure 3B).

Although noninvasive measures of pulmonary and RV pressures are helpful, serial measurements of RV function remain key to improving the translational applicability of preclinical studies in mice. The most extensively studied echocardiographic parameters of RV function that are of proven clinical utility in

humans are TAPSE, s' , MPI, and FAC.⁵ We measured TAPSE, a marker of longitudinal RV systolic function⁸ that also correlates with measures of global systolic function in PH.⁹ TAPSE was recorded in control mice as 1.06 ± 0.04 mm ($n=8$), similar to readings previously published under baseline conditions.¹⁰ In contrast, TAPSE was 0.79 ± 0.05 mm in bleomycin mice ($n=8$; $P=0.003$) (Figure 3C); this significant decrease is reflective of decreased RV longitudinal systolic function in the bleomycin mice. We next measured s' , ensuring correct basal to annular Doppler alignment. s' was also consistently reduced in bleomycin-treated mice (control: 29.19 ± 1.3 mm/s [$n=8$]; versus bleomycin: 21.29 ± 1.2 mm/s [$n=8$]; $P < 0.001$) (Figure 3D). MPI is a measure of global RV systolic function and diastolic function, and is a strong predictor of clinical course and survival in patients with PH.¹¹ Measurement of MPI was performed using tissue Doppler, calculated using a single view. Alterations in heart rate may significantly impact isovolumetric relaxation time and isovolumetric contraction time, and by association MPI; therefore, care was taken to ensure heart rates were maintained within a narrow range (400–450 beats per minute). MPI was significantly elevated in bleomycin mice (0.51 ± 0.03 ; $n=8$) compared with control (0.37 ± 0.01 ; $n=7$; $P=0.006$) (Figure 3E). FAC, a measurement that in contrast to TAPSE incorporates both the longitudinal and transversal components of RV contraction, strongly associates with RV ejection fraction and is an important prognostic tool in patients with PH.¹²

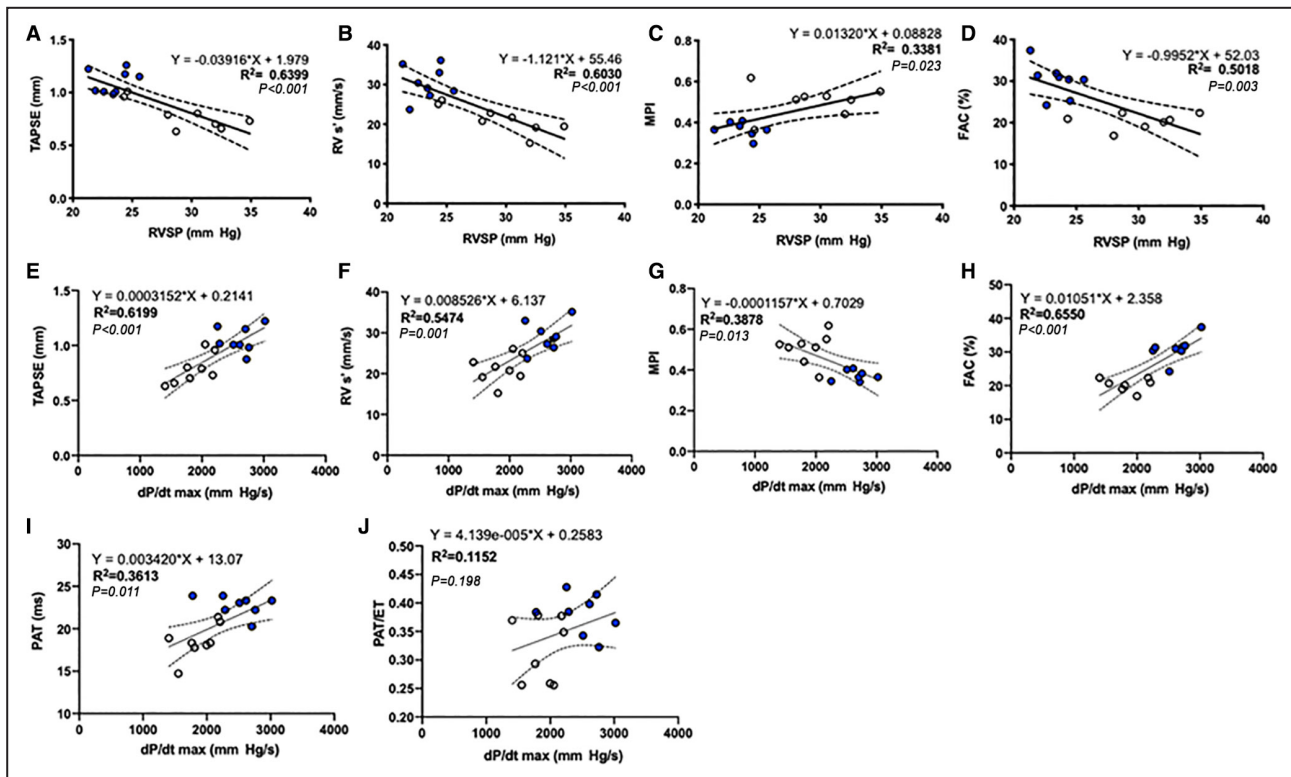


Figure 5. Comparative correlation of novel and previously validated echocardiographic measures of pulmonary pressure and RV function with invasively measured RVSP and maximum change pressure/change time (dP/dt max).

(Top) Correlation between RVSP and novel echocardiographic measures measured at 21 days: TAPSE (n=16) (A), RV peak systolic myocardial velocity (s') (n=16) (B), MPI (n=15) (C), and FAC (n=15) (D). (Middle) Correlation between dP/dt max and TAPSE (n=16) (E), s' (n=16) (F), MPI (n=15) (G), and FAC (n=15) (H). (Bottom) Correlation between dP/dt max and PAT (n=17) (I) and PAT/ET (n=17) (J). Statistical analysis was performed using the Pearson correlation coefficient (R) to evaluate linear correlations, and expressed as its square (R^2). Control mice shown in blue circles, and bleomycin-treated mice shown in gray circles. ET indicates ejection time; FAC, fractional area change; MPI myocardial performance index; PAT, pulmonary acceleration; RV, right ventricular; RVSP, RV systolic pressure; and TAPSE tricuspid annular plane systolic excursion.

Measurement in the 4-chamber view yielded significantly reduced values in FAC in the bleomycin-treated mice (20.3 ± 0.7 ; n=7) compared with control (31.0 ± 1.3 ; n=8; $P < 0.001$) (Figure 3F). Together, the demonstrated significant effect of bleomycin on the above measures is supportive of their value in measuring RV function in murine models. Baseline RV echocardiographic measures were recorded and compared with corresponding measurements at 3 weeks. There were statistically significant differences in 3-week measurements among bleomycin-treated mice in TAPSE (day 0: 0.99 ± 0.04 mm [n=5]; versus day 21: 0.84 ± 0.06 mm/s [n=5]; $P = 0.018$), s' (day 0: 27.74 ± 1.01 mm/s [n=5]; versus day 21: 22.56 ± 1.30 mm/s [n=5]; $P = 0.024$), and FAC (day 0: 28.96 ± 2.12 mm/s [n=5]; versus day 21: 19.38 ± 0.93 mm/s [n=4]; $P = 0.046$), which were not observed in the control cohort (Figure 3G through 3J). There was a similar trend in MPI, which did not reach statistical significance (day 0: 0.33 ± 0.03 [n=5]; versus day 21: 0.51 ± 0.04 [n=8]; $P = 0.076$), although there was a significant interaction between time and bleomycin

treatment observed ($P = 0.002$). Both s' ($P < 0.001$) and FAC ($P = 0.013$) also exhibited a significant interaction between treatment and time, whereas for TAPSE, there was no statistical significance reached across the time course of the experiment.

Interobserver and Intraobserver Variability

For TAPSE, s', MPI, and FAC intraobserver variability, the bias was 3.4%, 0.4%, 0.7%, and 1.5%, respectively; the 95% limits of agreement were -11.9 and 18.8 mm, -9.9 and 10.7 mm/s, -20.2% and 19.9%, and -12.0 and 15.1, respectively; and the intraclass correlation coefficients were 0.93, 0.96, 0.91, and 0.91, respectively (Figure 4A through 4D). For interobserver variability, the bias was -0.3, 7.4, 4.5, and 3.4, respectively; the 95% limits of agreement were -22.1 to 21.5, -10.2 to 25.1, -29.4 to 38.4, and -25.4 to 32.3, respectively; and the intraclass correlation coefficients were 0.92, 0.94, 0.58, and 0.75, respectively (Figure 4E through 4H).

Correlation of RV Echocardiographic Measures With Invasive Measurements of RVSP and dP/dt Max

We examined the association of TAPSE, s', MPI, and FAC with invasive measures of pulmonary pressures and RV systolic contractility, as measured by RVSP and dP/dt max. All 4 measures correlated with RVSP: TAPSE ($R^2=0.6399$; $P<0.001$), s' ($R^2=0.6030$; $P<0.001$), MPI ($R^2=0.3381$; $P=0.023$), and FAC ($R^2=0.5018$; $P=0.003$) (Figure 5A through 5D). In comparison to RVSP, RV dP/dt max represents the maximal rate of pressure increase in the right ventricle. This is an invasive and validated index of both contractility and prognosis.¹³ dP/dt max correlated strongly with TAPSE ($R^2=0.6199$; $P<0.001$), s' ($R^2=0.5474$; $P=0.001$), MPI ($R^2=0.3878$; $P=0.013$), and FAC ($R^2=0.6550$; $P<0.001$) (Figure 5E through 5H). These relationships were stronger than dP/dt max to PAT ($R^2=0.3613$; $P=0.01$) and PAT/ET ($R^2=0.1152$; $P=0.198$) (Figure 5I through 5J). It is notable that these linear regression relationships were only evident when the 2 groups were analyzed as a single cohort. When individual group linear regression was plotted, most significant correlations between hemodynamic and echocardiography parameters were lost, likely related to the homogeneity of data within groups and reduced power (Table).

Sensitivity and Specificity of RV Echocardiographic Parameters for Detection of Systolic Contractility

We next sought to establish the diagnostic performance of the noninvasive echocardiographic

parameters for identifying RV dysfunction, defined by $dP/dt \max \leq 2100$ mmHg/s. Receiver operating characteristic curves demonstrated that TAPSE (<0.84 mm), s' (<23.3 mm/s), MPI (>42.4), and FAC ($<23.3\%$) predicted reduced systolic function with high precision (sensitivity/specificity for TAPSE: 83%/90%; s': 83%/90%; MPI: 83%/78%; and FAC: 100%/89%; Figure 6A through 6D).

Invasive pressure-volume analysis was also conducted and confirmed significant RV dysfunction in bleomycin-treated mice (Figure 7), where higher RVSP was accompanied by reduced stroke volume and cardiac output in the bleomycin-treated mice. In these same mice, echocardiographically measured PAT/ET was lower in bleomycin-treated mice and correlated with cardiac output.

DISCUSSION

The echocardiographic parameters of RV function that have been developed and used clinically in human echocardiography are yet to be widely applied in mouse disease models. Herein, we demonstrate the feasibility of using high-resolution murine echocardiography to measure TAPSE, s', MPI, and FAC in a murine model of group III PH, with excellent interobserver and intraobserver reproducibility, and strong correlation with invasive measures of both RV systolic pressure and contractility. Our results show, for the first time, that TAPSE, s', MPI, and FAC are strongly correlated with invasive measures of RV function. This is an important advance given that RV function and its response to pressure overload is the major driver of adverse outcomes in clinical practice. This illustrates

Table. Linear Regression Analysis Between Hemodynamic and Echocardiography Parameters

Linear regression parameters		Control			Bleomycin			Figure
x Axis	y Axis	R ²	P value	n	R ²	P value	n	
RVSP	TAPSE	0.063	0.548	8	0.587	0.027*	8	5A
RVSP	s'	0.008	0.828	8	0.662	0.014*	8	5B
RVSP	MPI	0.141	0.407	7	0.011	0.086	8	5C
RVSP	FAC	0.167	0.314	8	0.070	0.567	7	5D
dP/dt max	TAPSE	0.010	0.814	8	0.515	0.045*	8	5E
dP/dt max	s'	0.128	0.384	8	0.067	0.538	8	5F
dP/dt max	MPI	0.001	0.939	7	0.014	0.784	8	5G
dP/dt max	FAC	0.307	0.155	8	0.022	0.751	7	5H
dP/dt max	PAT	0.190	0.241	9	0.415	0.085	8	5I
dP/dt max	PAT/ET	0.093	0.462	8	0.001	0.934	8	5J
CO	PAT/ET	0.074	0.514	8	0.209	0.439	5	7G

CO indicates cardiac output ($\mu\text{L}/\text{min}$); dP/dt, maximum change pressure/change time ($\Delta\text{mmHg}/\Delta\text{s}$); ET, ejection time; FAC, fractional area change (%); MPI, myocardial performance index; PAT, pulmonary acceleration time (ms); s', right ventricular peak systolic myocardial velocity (mm/s); RVSP, right ventricular systolic pressure (mmHg); and TAPSE, tricuspid annular plane systolic excursion (mm).

* $P<0.05$, statistically significant vs control.

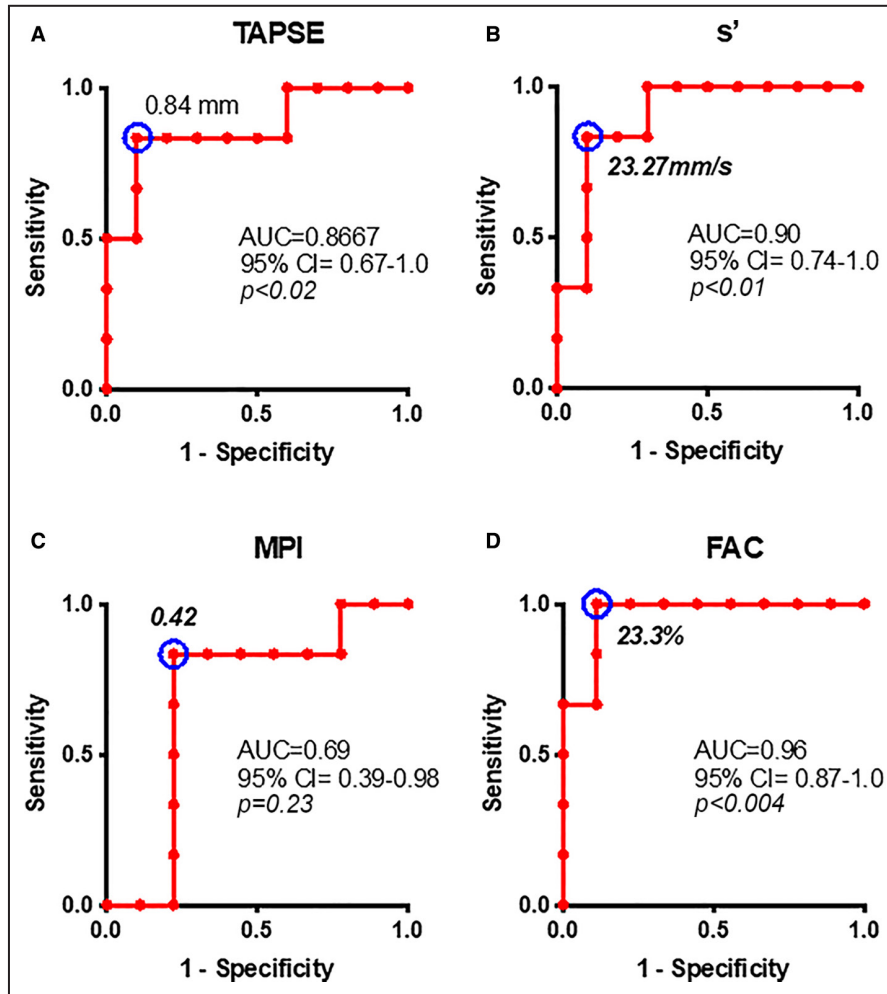


Figure 6. Sensitivity and specificity of RV echocardiographic measures for maximum change pressure/change time (dP/dt max).

Receiver operating characteristic curves demonstrating sensitivity and specificity of TAPSE (A), RV peak systolic myocardial velocity (s') (B), MPI (C), and FAC (D) for detecting RV dysfunction, as defined by dP/dt max <2100 mmHg/s. AUC and 95% CIs are displayed, as well as optimal cutoff values (blue circle), calculated using the Youden index. AUC indicates area under the curve; FAC, fractional area change; MPI, myocardial performance index; RV, right ventricular; and TAPSE, tricuspid annular plane systolic excursion.

that these noninvasive measures hold strong promise as tools to longitudinally track RV dysfunction in pre-clinical research.

These measures have previously been investigated in healthy C57BL/6 and CD1 mice.¹⁰ However, they have not been assessed and validated in disease models of PH. Some of the measures have been used and shown to reflect PH secondary to left ventricular dysfunction induced by myocardial infarction.¹⁴ However, the effects of left anterior descending coronary artery ligation and left ventricular dysfunction on ventricular-vascular coupling, septal bowing, and RV biomechanics and physiology could lead to markedly different RV functional results.¹⁴ Therefore, independent measurement and validation performed in this study in the

more commonly studied bleomycin mouse model is of paramount importance for validating the future use of these RV parameters. The results presented now allow for increased statistical power with recording of intraindividual changes in serial measurements, thereby minimizing animal use.

TAPSE has an excellent correlation with RV ejection fraction in different types of chronic PH. It is relatively easy to measure, it is reproducible, its value is closely correlated with invasive hemodynamic measurements, and it predicts survival in a mixed cohort of patients with pulmonary arterial hypertension.¹⁵ However, TAPSE assumes that the displacement of the basal and adjacent segments in the apical 4-chamber view is representative of the function of

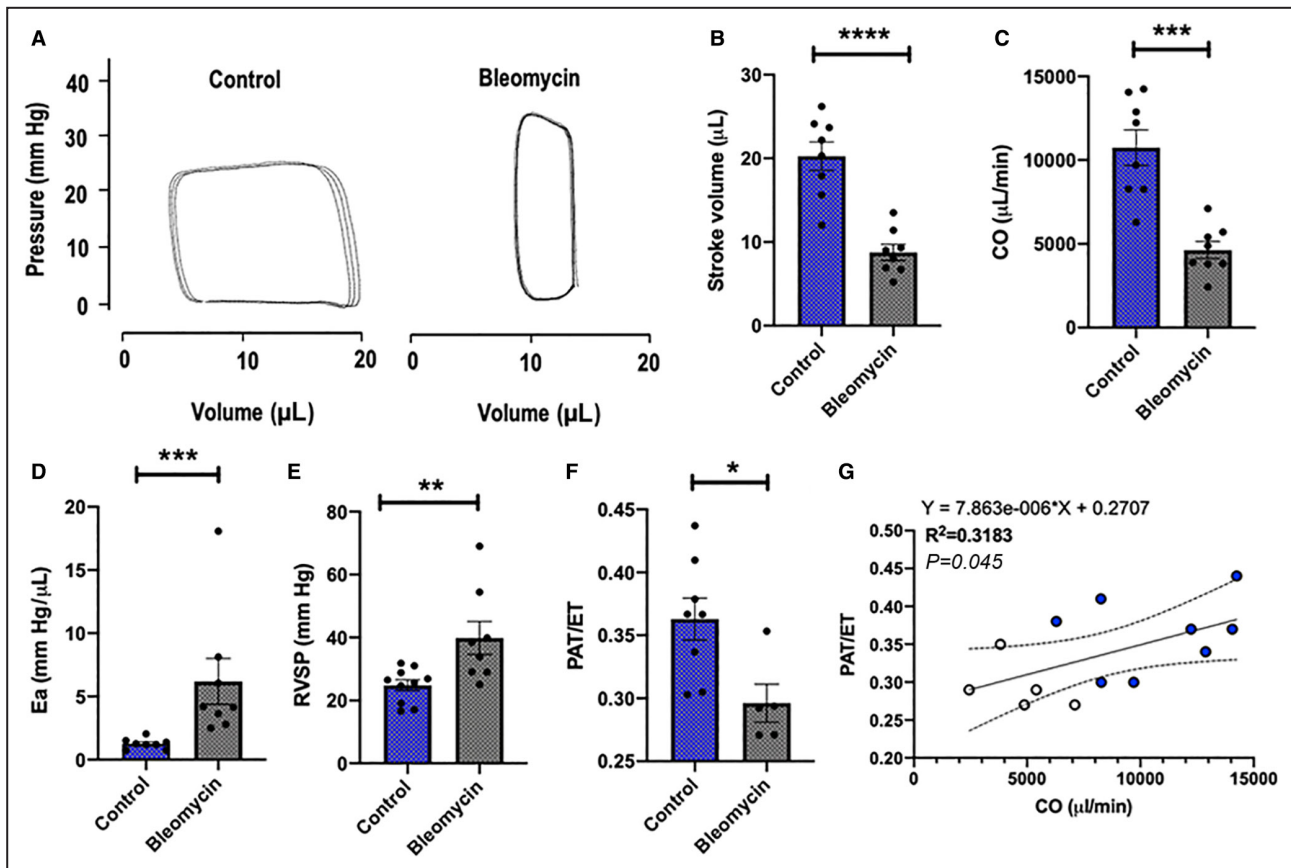


Figure 7. Pressure-volume loop analysis confirms RV dysfunction in BLEO-treated mice.

Representative RV pressure-volume loops from control and BLEO-treated mice (A), with summary data of stroke volume (control, n=8; BLEO, n=8) (B), CO (C) (control, n=8; BLEO, n=8), Ea (D) (control, n=8; BLEO, n=8), and RVSP (E) (control, n=10; BLEO, n=8) are shown. In the same mice, PAT over ET (F) (control, n=8; BLEO, n=5) is shown and correlates with CO (G). Data shown are mean±SEM. Statistical analysis was performed using unpaired Student *t* tests (B through F) or simple linear regression. **P*<0.05, ***P*<0.01, ****P*<0.001, and *****P*<0.0001 vs control. Ea indicates arterial elastance; BLEO, bleomycin; CO, cardiac output; ET, ejection time; PAT, pulmonary acceleration time; and RV right ventricular.

the entire RV, which is invalid in disease states with regional wall motion abnormalities.⁵ RV MPI is a global estimate of systolic and diastolic function in the RV that has likewise shown predictive value in future events in patients with PH.¹⁶ We demonstrated that MPI is increased in mice with PH, reflecting impaired systolic and diastolic function. Receiver operating characteristic curve analysis demonstrated high sensitivity and specificity for prediction of RV dysfunction. However, measurements of MPI did yield higher intraobserver and interobserver variability compared with TAPSE, *s'*, and FAC. It is not entirely clear why MPI did not correlate as strongly with invasive contractile function as other echocardiographic measures. However, elevated right atrial pressure is theoretically plausible in this PH model and is known to artifactually decrease MPI,⁵ potentially decreasing its reliability as a measure of contractility and thus providing a possible explanation for the lesser associations.

Measures of RV systolic function, like RV strain and strain rate, have potential to improve serial measures in preclinical models of PH. RV global and longitudinal strain and strain rate correlate strongly with RV dysfunction in patients with pulmonary arterial hypertension¹⁷ and are believed to be preferable to TAPSE because they are not affected by heart motion. However, acquisition of images suitable for strain analysis of the RV is currently technically challenging in mice, as it is difficult to obtain clear windows of a well-delineated RV free wall needed for accurate strain calculation.

We also found *s'* measurements to be a measure of RV dysfunction. Our measurements were lower than those found by previous groups using control C57BL6 mice.¹⁰ However, it also showed the highest intraclass correlation coefficient when compared with TAPSE and MPI. A plausible explanation to account for higher results reported in the literature could be falsely high measurements attributable to overgain of the Doppler envelope.

As previously alluded to, although the invasively measured pulmonary arterial pressure waveform is a valuable diagnostic tool in PH, it has limited prognostic value and is not ideally suited as the gold standard for validation of RV functional parameters. RV dP/dt correlates strongly with RV ejection fraction and is therefore a representative marker of RV function. However, RV dP/dt is load dependent, and impacted by severe tricuspid regurgitation, which is a structural abnormality that cannot be excluded in the context of PH-induced RV dilatation. Moreover, tricuspid regurgitation is difficult to assess echocardiographically in mice. Although our pressure-volume analysis supports the proof of concept, we have not yet been able to correlate RV pressure-volume data with simultaneous 4-chamber echocardiography analysis, and this is an aim of a future study.

A further limitation of this study is that cardiac magnetic resonance imaging was not performed, and although we performed preliminary analysis of RV pressure-volume loops, we were unable to consistently obtain data of high enough quality for more complex analysis. Measurements of RV function and RV cardiomyocyte efficiency, derived from simultaneous acquisition of RV pressure and volume data, including end-systolic ventricular elastance and ventricular-arterial coupling, correlate strongly with P and its progression^{18,19} and would be valuable adjuncts in the validation of novel measures of PH-induced RV dysfunction. We have demonstrated the application of RV echocardiographic measures as they pertain to mice with group III PH; however, given the heterogeneous pathophysiology of PH, these results may not be directly translatable to alternate mouse models of PH. Caution should also be made about the correlation analysis of echocardiographic and pulmonary catheterization measurements because of the possibility of Simpson bias. This is particularly important when examining relationships across 2 distinct groups with no overlap, and with considerable homogeneity within the groups. However, as seen in [Figure 5](#) and [7G](#), there is some heterogeneity within each group, and some overlap of the groups.

In conclusion, our findings demonstrate that the noninvasive echocardiographic measures of TAPSE, s', MPI, and FAC accurately identify both PH and RV dysfunction in mice. These robust measures for detection of RV dysfunction in murine group III PH offer the opportunity for improved therapeutic testing with serial measurements and are therefore of value in preclinical PH research.

ARTICLE INFORMATION

Received July 9, 2020; accepted September 2, 2022.

Affiliations

Sydney Medical School, The University of Sydney, New South Wales, Sydney, Australia (T.S.H., K.J.B., M.U., G.A.F.); The Kolling Institute, Royal North Shore Hospital, New South Wales, Sydney, Australia (T.S.H., K.J.B., M.U., G.A.F.); Dept. of Physiology, Biomedicine Discovery Institute, Faculty of Medicine, Nursing and Health Sciences, Monash University, Clayton, Australia (K.J.B.); Cardiology Division, Department of Internal Medicine, University of Texas Southwestern Medical Center, Texas, Dallas, USA (G.G.S.); Department of Advanced Biomedical Sciences, Federico II University, Naples, Italy (G.G.S.); Westmead Hospital, Faculty of Medicine, University of Sydney, New South Wales, Australia (T.C.T.); and Department of Cardiology, Blacktown Hospital, New South Wales, Blacktown, Australia (T.C.T.).

Acknowledgments

The authors acknowledge the facilities and the scientific and technical assistance of Elizabeth Blanchard and Nana Sunn of Sydney Imaging, a Core Research Facility, University of Sydney.

Sources of Funding

This work is supported by the National Health and Medical Research Council (NHMRC) of Australia practitioner fellowship (Dr Figtree; APP1135920) and an NHMRC equipment grant.

Disclosures

The authors have no disclosures to report.

REFERENCES

- Hoepfer MM, Bogaard HJ, Condliffe R, Frantz R, Khanna D, Kurzyna M, Langleben D, Manes A, Satoh T, Torres F, et al. Definitions and diagnosis of pulmonary hypertension. *J Am Coll Cardiol*. 2013;62:D42–D50. doi: 10.1016/j.jacc.2013.10.032
- Ryan JJ, Archer SL. The right ventricle in pulmonary arterial hypertension: disorders of metabolism, angiogenesis and adrenergic signaling in right ventricular failure. *Circ Res*. 2014;115:176–188. doi: 10.1161/CIRCRESAHA.113.301129
- Vonk-Noordegraaf A, Haddad F, Chin KM, Forfia PR, Kawut SM, Lumens J, Naeije R, Newman J, Oudiz RJ, Provencher S, et al. Right heart adaptation to pulmonary arterial hypertension: physiology and pathobiology. *J Am Coll Cardiol*. 2013;62:D22–D33. doi: 10.1016/j.jacc.2013.10.027
- Bubb KJ, Trinder SL, Baliga RS, Patel J, Clapp LH, MacAllister RJ, Hobbs AJ. Inhibition of phosphodiesterase 2 augments cGMP and cAMP signaling to ameliorate pulmonary hypertension. *Circulation*. 2014;130:496–507. doi: 10.1161/CIRCULATIONAHA.114.009751
- Rudski LG, Lai WW, Afilalo J, Hua L, Handschumacher MD, Chandrasekaran K, Solomon SD, Louie EK, Schiller NB. Guidelines for the echocardiographic assessment of the right heart in adults: a report from the American Society of Echocardiography endorsed by the European Association of Echocardiography, a registered branch of the European Society of Cardiology, and the Canadian Society of Echocardiography. *J Am Soc Echocardiogr* 2010;23:685–713; quiz 786–8.
- Parasuraman S, Walker S, Loudon BL, Gollop ND, Wilson AM, Lowery C, Frenneaux MP. Assessment of pulmonary artery pressure by echocardiography—a comprehensive review. *Int J Cardiol Heart Vasc*. 2016;12:45–51. doi: 10.1016/j.ijcha.2016.05.011
- Thibault HB, Kurtz B, Raheer MJ, Shaik RS, Waxman A, Derumeaux G, Halpern EF, Bloch KD, Scherrer-Crosbie M. Noninvasive assessment of murine pulmonary arterial pressure: validation and application to models of pulmonary hypertension. *Circ Cardiovasc Imaging*. 2010;3:157–163. doi: 10.1161/CIRCIMAGING.109.887109
- Carlsson M, Ugander M, Heiberg E, Arheden H. The quantitative relationship between longitudinal and radial function in left, right, and total heart pumping in humans. *Am J Physiol Heart Circ Physiol*. 2007;293:H636–H644. doi: 10.1152/ajpheart.01376.2006
- Saxena N, Rajagopalan N, Edelman K, Lopez-Candales A. Tricuspid annular systolic velocity: a useful measurement in determining right ventricular systolic function regardless of pulmonary artery pressures. *Echocardiography*. 2006;23:750–755. doi: 10.1111/j.1540-8175.2006.00305.x
- Kohut A, Patel N, Singh H. Comprehensive echocardiographic assessment of the right ventricle in murine models. *J Cardiovasc Ultrasound*. 2016;24:229–238. doi: 10.4250/jcu.2016.24.3.229

11. Tei C, Dujardin KS, Hodge DO, Bailey KR, McGoon MD, Tajik AJ, Seward SB. Doppler echocardiographic index for assessment of global right ventricular function. *J Am Soc Echocardiogr*. 1996;9:838–847. doi: [10.1016/S0894-7317\(96\)90476-9](https://doi.org/10.1016/S0894-7317(96)90476-9)
12. Hoette S, Creuze N, Gunther S, Montani D, Savale L, Jais X, Parent F, Sitbon O, Rochitte CE, Simonneau G, et al. RV fractional area change and TAPSE as predictors of severe right ventricular dysfunction in pulmonary hypertension: a CMR study. *Lung*. 2018;196:157–164. doi: [10.1007/s00408-018-0089-7](https://doi.org/10.1007/s00408-018-0089-7)
13. Morimont P, Lambermont B, Desai T, Janssen N, Chase G, D'Orio V. Arterial dP/dtmax accurately reflects left ventricular contractility during shock when adequate vascular filling is achieved. *BMC Cardiovasc Disord*. 2012;12:13.
14. Bellofiore A, Chesler NC. Methods for measuring right ventricular function and hemodynamic coupling with the pulmonary vasculature. *Ann Biomed Eng*. 2013;41:1384–1398. doi: [10.1007/s10439-013-0752-3](https://doi.org/10.1007/s10439-013-0752-3)
15. Forfia PR, Fisher MR, Mathai SC, Houston-Harris T, Hemnes AR, Borlaug BA, Chamara E, Corretti MC, Champion HC, Abraham TP, et al. Tricuspid annular displacement predicts survival in pulmonary hypertension. *Am J Respir Crit Care Med*. 2006;174:1034–1041. doi: [10.1164/rccm.200604-547OC](https://doi.org/10.1164/rccm.200604-547OC)
16. Sebbag I, Rudski LG, Therrien J, Hirsch A, Langleben D. Effect of chronic infusion of epoprostenol on echocardiographic right ventricular myocardial performance index and its relation to clinical outcome in patients with primary pulmonary hypertension. *Am J Cardiol*. 2001;88:1060–1063. doi: [10.1016/S0002-9149\(01\)01995-6](https://doi.org/10.1016/S0002-9149(01)01995-6)
17. Li Y, Xie M, Wang X, Lu Q, Fu M. Right ventricular regional and global systolic function is diminished in patients with pulmonary arterial hypertension: a 2-dimensional ultrasound speckle tracking echocardiography study. *Int J Cardiovasc Imaging*. 2013;29:545–551. doi: [10.1007/s10554-012-0114-5](https://doi.org/10.1007/s10554-012-0114-5)
18. Fourie PR, Coetzee AR, Bolliger CT. Pulmonary artery compliance: its role in right ventricular-arterial coupling. *Cardiovasc Res*. 1992;26:839–844. doi: [10.1093/cvr/26.9.839](https://doi.org/10.1093/cvr/26.9.839)
19. Vanderpool RR, Pinsky MR, Naeije R, Deible C, Kosaraju V, Bunner C, Mathier MA, Lacomis J, Champion HC, Simon MA. RV-pulmonary arterial coupling predicts outcome in patients referred for pulmonary hypertension. *Heart*. 2015;101:37–43. doi: [10.1136/heartjnl-2014-306142](https://doi.org/10.1136/heartjnl-2014-306142)